IN-FLIGHT THRUST DETERMINATION ON A REAL-TIME BASIS

FINAL REPORT

PRINCIPAL INVESTIGATORS

Ronald J. Ray

Tom Carpenter

Doral R. Sandlin

April 1984

California Polytechnic State University

Aeronautical Engineering Department

San Luis Obispo, California

Grant No. NCC4-1

ABSTRACT

IN-FLIGHT THRUST DETERMINATION ON A REAL-TIME BASIS

Ronald J. Ray

April 1984

A real-time computer program was implemented on a F-15 jet fighter to monitor in-flight engine performance of a Digital Electronic Engine Controlled (DEEC) F-100 engine.

This thesis describes the application of two gas generator methods to calculate in-flight thrust real-time at the NASA Dryden Flight Research Facility. A comparison was made between the actual results and those predicted by an engine model simulation. The percent difference between the two methods was compared to the predicted uncertainty based on instrumentation and model uncertainty and agreed closely with the results found during altitude facility testing. Data was obtained from acceleration runs of various altitudes at maximum power settings with and without afterburner.

Real-time in-flight thrust measurement was a major advancement to flight test productivity and was accomplished with no loss in accuracy over previous post flight methods.

TABLE OF CONTENTS

LIST OF TABLES

LIST OF FIGURES

---

* These figures were taken in whole or part from excerpts of the DEEC Mini Symposium held May 24-25, 1984, at the NASA Dryden Research Facility, Edwards, California. All materials were originated by the author.

NOMENCLATURE

AJ	Nozzle Area
C	Speed of Sound
CG	Gross Thrust Coefficient
CV	Nozzle Velocity Coefficient
CIVV	Compressor Inlet Variable Vanes
DEEC	Digital Electronic Engine Control
EPR	Engine Pressure Ratio (PT7/P0)
g	Gravity Constant
FG	Gross Thrust
FGI	Ideal Gross Thrust
FLIDAB	Flight Data Base
FN	Net Thrust
FR	Ram Drag
MI	Ideal Mach Number
N1	Fan Speed
P0	Free Stream Static Pressure
PS2	Static Pressure Station Two
PT6M	Measured Total Pressure Station Six
PT7	Total Pressure Station Seven
PTA	Total Pressure-Area Method
R	Gas Constant
RCIVV	Rear Compressor Inlet Variable Vanes
T7	Temperature Station Seven
TT2	Total Temperature Station Two
TT7	Total Temperature Station Seven

Nomenclature, Continued

TTW	Total Temperature-Weight Flow Method
U	Uncertainty
V	Velocity
VT	Velocity at Nozzle Throat (Station Seven)
WAT	Total Airflow
WFAC	Afterburner Core Fuel Flow
WFAD	Afterburner Duct Fuel Flow
WFGG	Gas Generator Fuel Flow
WFT	Total Fuel Flow
WG6	Gas Flow Rate Station Six
WG7	Gas Flow Rate Station Seven
XPR	Nozzle Pressure Ratio
γ	Specific Heat Coefficient Ratio

INTRODUCTION

One of the most important objectives in any flight test program is the measure of performance. This has typically been a difficult and time consuming task that has sometimes delayed important flight tests. The result of this problem has caused loss of man hours, delays between flights and increased cost. Advancements in computer capacity and capability has drastically reduced the time required for performance evaluation and made possible real-time in-flight measurement.

The NASA Dryden Flight Research Facility has been involved in a flight test program with a Digital Electronic Engine Control (DEEC) on a F-15 airplane. One of the objectives of this program is the evaluation of the airframe, propulsion and computer system integration. Of particular importance is the performance analysis. To aid in this analysis a real-time computer program that calculates the internal thrust developed by the F-100 engine in-flight has been implemented. This program allows the engineer to accurately monitor gross thrust, net thrust, ram drag and specific fuel consumption instantaneously from a control room during test flights.

To calculate thrust, two gas generator methods were employed. These methods described in References 1 and 2, have been studied and proven to be feasible and accurate. Because of the instrumentation already available from the DEEC engine and airframe system no special instrumentation was required. The software used was a condensed version of the manufacturer's supplied engine performance deck (Reference 3) modified to run real-time.

Comparisons between the two gas generator methods and predicted values were made to verify accuracy. Data was primarily obtained from constant power setting acceleration runs at a variety of conditions. Unsteady throttle transient data was also analyzed. An uncertainty analysis was used to compare the differences between the two gas generator methods and confirm the accuracy of both methods.

DESCRIPTION OF APPARATUS

Airplane

The F-15 airplane is a high performance twin-engine fighter with a Mach number capability of 2.5. The engine inlets are two-dimensional external compression type with three ramps (Figure 1), and feature variable capture area described in Reference 4.

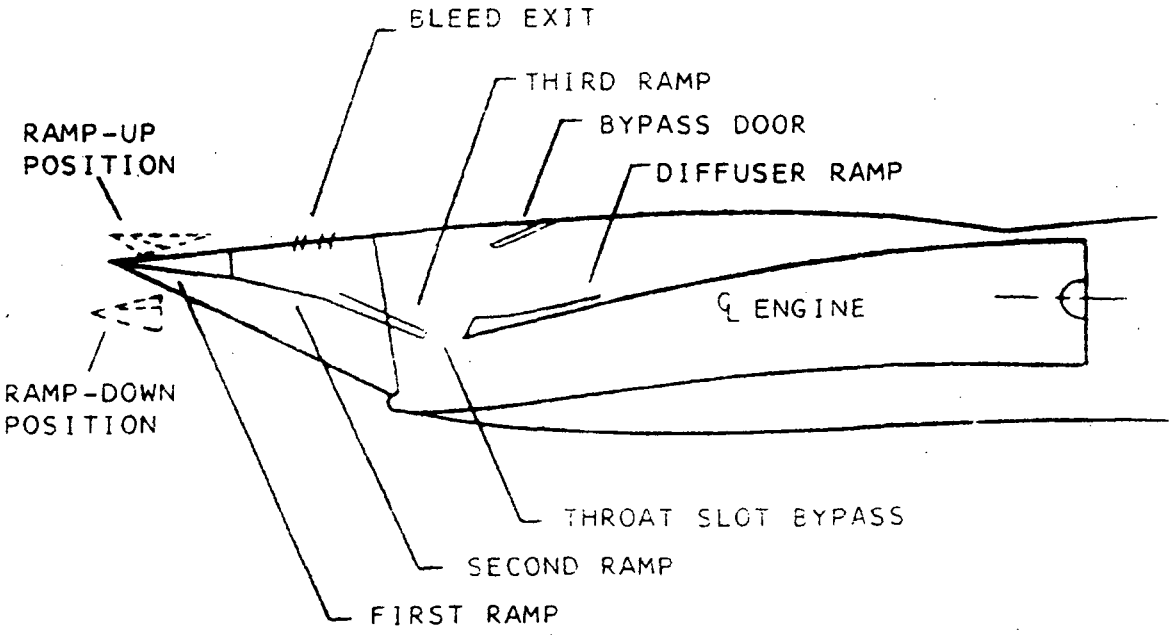

Figure 1: F-15 Engine Inlet

The aircraft used had been modified to be a general flight test bed. The specific modification for the DEEC flight test program was replacement of the left engine with the DEEC equipped test engine and appropriate DEEC/fuel cooling modifications.

Engine Description

The F-100 engine is a twin-spool, low bypass ratio, afterburning turbofan of the 25,000 pound thrust class. Figure 2 shows the designated engine stations. The three-stage fan is driven by a low pressure, two-stage turbine and the ten-stage high pressure compressor is driven by a two-stage high pressure turbine. To increase fan efficiency and achieve high performance over a wide range of operating conditions the engine incorporates compressor inlet variable vanes (CIVV) and rear compressor variable vanes (RCVV). Continuously variable thrust augmentation is provided by a mixed-flow afterburner. The augmentor incorporates five spray ring segments which are ignited sequentially. This allows variable afterburner thrust. High energy gas is exhausted through a variable-area, convergent-divergent nozzle of the balance beam design that enables simultaneous optimization of nozzle area, expansion ratio and boattail or aftend drag.

The major contributors to the high performance of the F-100 engine are high aerodynamic stage loadings, high-temperature turbines with advanced cooling features, variable internal aerodynamics, high strength-to-weight alloys and a light-weight balanced beam exhaust nozzle. Information on the design and development of the F-100 engine can be found in References 4 and 5.

The primary flight test engine used during initial testing of the Digital Electronic Engine Control and for calculation of real-time thrust was designated P680063. This engine was one of two prototype F100-PW-100 engines that were calibrated for thrust and airflow in the NASA Lewis Research Center Propulsion Systems Laboratory 4 altitude facility. The performance of this engine determined at the NASA Lewis facility is described in References 6 and 7.

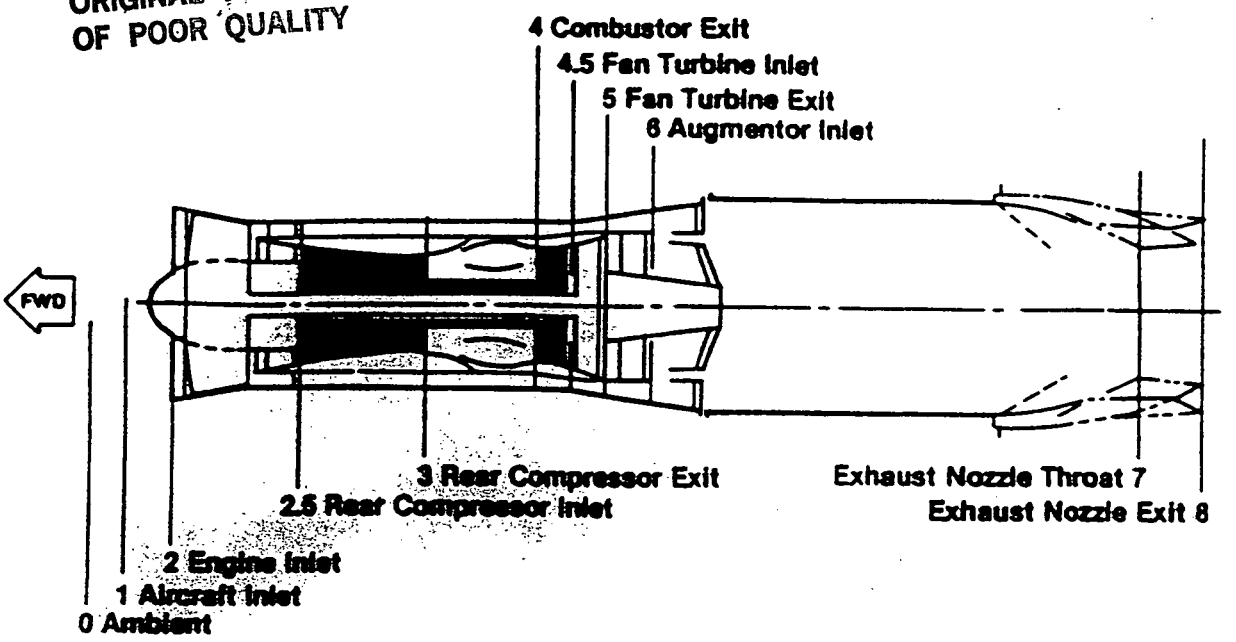

Figure 2. F-100 Engine Stations

Digital Electronic Engine Control

The DEEC is a full-authority, engine mounted digital electronic control system that performs the functions of the standard F-100 engines hydromechanical unified fuel control and supervisory digital engine electronic control. Its logic provides open loop scheduling of CIVV, RCIVV, start bleed position, and augmentor controls. The DEEC incorporates closed-loop control logic to eliminate the need for periodic trimming and to improve performance. Reference 8 gives a more complete description of the DEEC system and its performance.

There are some important advantages of having the DEEC available to supply engine data for the calculation of thrust. All of the parameters required to calculate thrust are available from the DEEC computer real-time and are measured with accurate, state-of-the-art instrumentation. In addition, the DEEC computer calculates airflow and pressure at station two, reducing the computational requirement on the ground.

Thrust Measurement Instrumentation on the DEEC Engine

The location of the engine instrumentation used in the calculation of in-flight thrust is shown in Figure 3. This instrumentation is common to the DEEC system and its associated data is available real-time from the DEEC computer. No special instrumentation was required and no modifications were made to any hardware for the calculation of in-flight thrust.

In addition to engine data, free stream static pressure, temperature, Mach number and altitude were available from the aircraft data system.

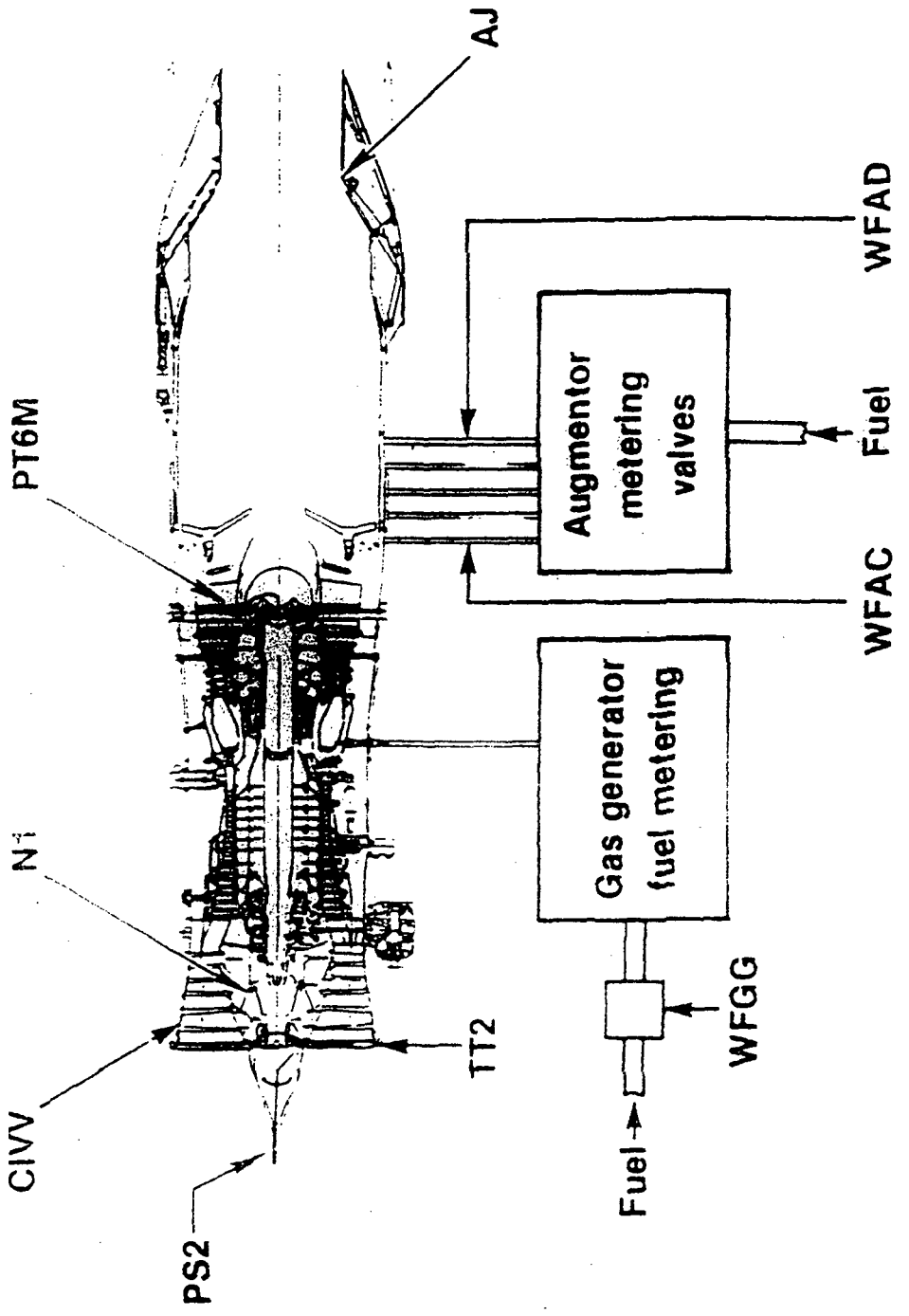

Figure 3. Thrust Measurement Instrumentation on DEEC Engine

PROCEDURE

Engine Performance Calculation

The software used to calculate in-flight thrust real-time is a modified version of the engine manufacturer's Fortran IV data reduction routine for determining in-flight performance and was intended for off-line analysis. The user's manual, Reference 3, gives a general description of the requirements to run the original program and its capabilities. In-flight gross thrust, net thrust and thrust specific fuel consumption are determined through correlation with mathematical model curves which are based on the altitude facility engine performance and measured thrust calibrations described by Reference 6.

The program uses two gas generator methods to calculate gross thrust, the total temperature and weight flow method (TTW) and the total pressure and area method (PTA), which differ mainly in the method used to calculate thrust. For both methods, the ideal gross thrust is defined as the thrust obtained when the flow at the primary nozzle is isentropically expanded to free-stream static pressure, that is:

$$FGI = \frac{WG7 * VI}{g}$$

The PTA equation is obtained by applying the continuity equation at the primary nozzle exit:

$$WG7 = V7 * A7 \frac{PT7}{R*T7}$$

Both equations rely on the ideal velocity being equal to the product of the ideal Mach number and the speed of sound,

$$VI = MI * c$$

where

$$MI = \sqrt{\left[\left(\frac{PT7}{P0}\right)^{\left(\frac{\gamma-1}{\gamma}\right)} - 1\right]\left(\frac{2}{\gamma-1}\right)}$$

and

$$C = \sqrt{\gamma * R * T * g}$$

The TTW equation is obtained by converting static temperature, T, to total temperature, TT, by using $\frac{TT}{T} = \left(\frac{PT}{P}\right)^{\left(\frac{\gamma-1}{\gamma}\right)}$ and simplifying, the ideal velocity becomes:

$$VI = \sqrt{TT7 \ \frac{2\,Rg}{\gamma-1} \ 1-\left(\frac{PT7}{P0}\right)^{\left(\frac{1-\gamma}{\gamma}\right)}}$$

Rearranging and simplifying these equations leads to the following resultant gross thrust equations:

$$FG(PTA) = PT7 * AJ * \gamma * \sqrt{\frac{2}{(\gamma-1)}\left(\frac{2}{\gamma+1}\right)^{\left(\frac{\gamma+1}{\gamma-1}\right)} 1-\left(\frac{PT7}{P0}\right)^{\left(\frac{1-\gamma}{\gamma}\right)}}\ CG$$

$$FG(TTW) = \frac{WG7}{g}\sqrt{TT7 * \frac{2Rc}{\gamma-1}}\sqrt{1-\left(\frac{PT7}{P0}\right)^{\left(\frac{1-\gamma}{\gamma}\right)}}\ CV$$

The final term is the correction factor from ideal to actual gross thrust and is obtained from empirical data. A more detailed development of these equations is found in References 2 and 9.

Net thrust is obtained by subtracting the ram drag force, FR, from the corrected gross thrust,

$$FR = \frac{WAT * V}{g}$$

$$FN = FG - FR$$

Because of the extreme temperature within the engine, many of the parameters necessary for the thrust calculation, such as exhaust pressures and temperatures, cannot be directly measured. These parameters are calculated from available instrumentation (Figure 3) by use of gas dynamic relationships and empirical mathematical models obtained during altitude facility testing described in Reference 6.

Gas Generator Method Calculation Flow

A schematic representation of the gas generator methods data flow and model calculations is given in Figure 4. The arrows show the flow of data. The blocks within the schematic illustrate the calculations performed. The model uses a combination of theoretical values, component test data, and full-scale engine data to generate the relationships necessary for the analysis. The engine core and afterburner sections are modeled separately as shown.

To model the engine core, first the mass flow change is calculated from the airflow and primary fuel-flow data supplied by the DEEC. The temperature rise is then calculated from the total temperature at station two and the fuel-to-air ratio in the core. The afterburner model calculates the change in total pressure, temperature and gas flow rate through this section. Once station seven is completely modeled, ideal gross thrust is calculated.

To correct the ideal thrust to actual, the model employs a nozzle analysis to calculate correction coefficients. The PTA method is corrected by the gross thrust coefficient, CG and the TTW method is corrected by the velocity coefficient, CV.

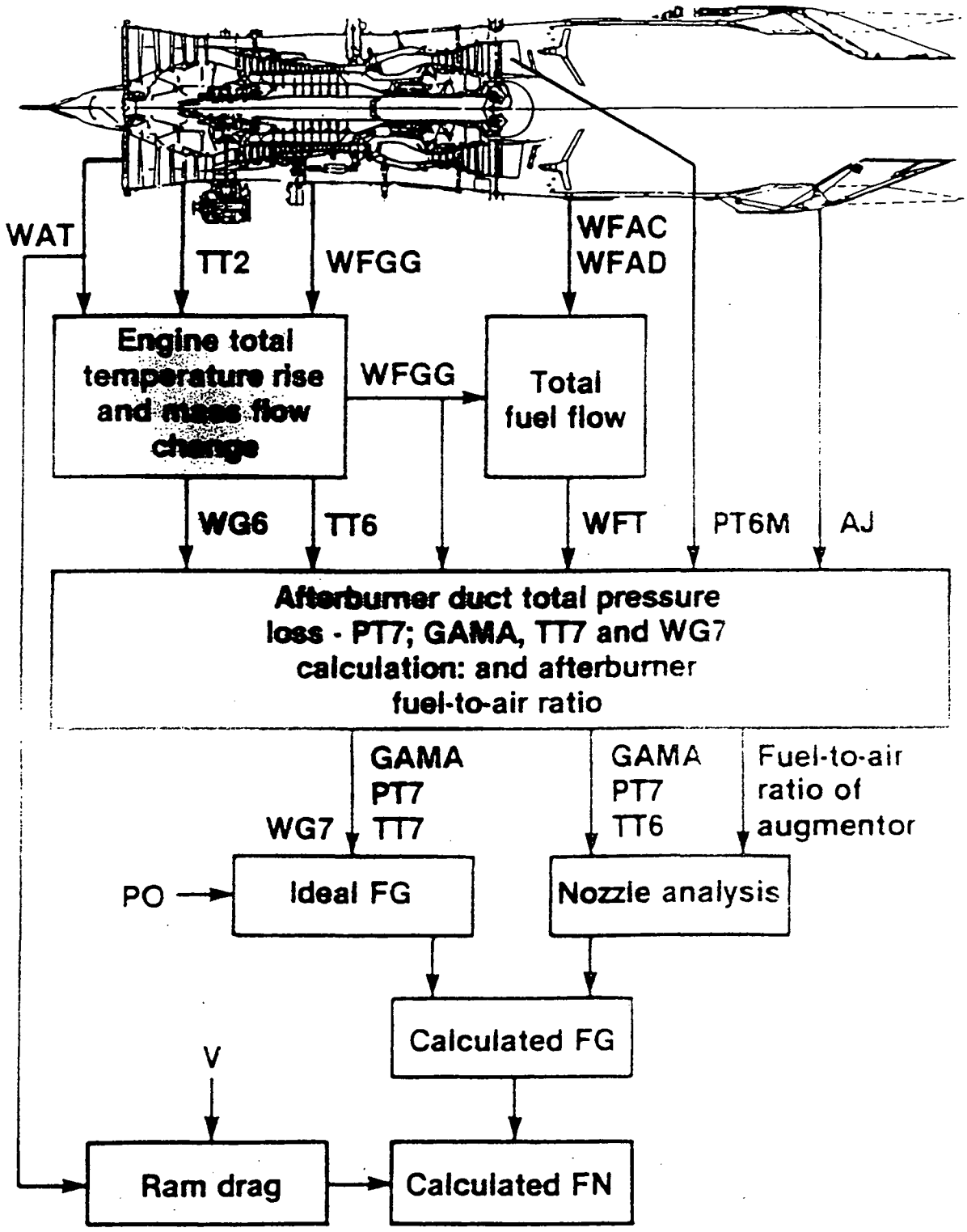

Figure 4. Gas Generator Method Calculation Flow

Modifications for Real-Time Operations

To increase the efficiency of the program and to meet real-time compatibility requirements the following modifications were made to the manufacturer's original post-flight program (Reference 3) in order to operate real-time.

1. The total airflow calculation was removed because of its availability from the DEEC.
2. The uncertainty logic was removed.
3. The output parameters were reduced to only the essential parameters requested for real-time display.
4. The method of inputting data was changed to allow instantaneous access from the main ground computer program.

These changes were primarily made to increase the speed of data reduction and no changes were made to the method of calculation other than more efficient programming.

The airflow calculation was actually an option in the original program. Because the DEEC engine computer calculates this parameter and supplied it on a real-time basis to the ground computer, the option was removed to eliminate the storage requirements of its five subroutines and the time consuming tests that were associated with the option. This in effect streamlined the program.

The removal of the uncertainty logic was an important factor in increasing the speed of the program. The original program analyzes the effect of each input parameter one at a time by looping back to the beginning of the program, varing a parameter by its uncertainty and repeating the performance calculation sequence to determining its associated uncertainty in thrust. Once all the independent thrust

uncertainties were determined, a root-sum-square calculation was made to find the overall uncertainty in thrust at the particular flight condition. This process was obviously time consuming and the results have little importance in the real-time environment. Removal of the uncertainty logic, including two subroutines and numerous logic tests, accounted for over a tenfold increase in the thrust computation speed.

In addition to the removal of the airflow and uncertainty logic, all other tests and calculations that were not essential to the calculation of gross and net thrust were removed and the output was reduced to only pertinent performance parameters for real-time display.

Both input and output methods were changed to allow instantaneous access of all parameters. This was accomplished by the use of the Fortran "common block" statement to instantly update input and output data as it varied. The "common block" statement was essential in meeting the requirement of real-time input and output compatibility.

All of the above mentioned modifications were made while allowing the performance program to run at its best rate of speed in the background of the main F-15/DEEC real-time computer program using taped data from previous flight test. To confirm that real-time computing rates were being achieved, a routine was added to monitor the rate thrust was calculated. Once the modifications were completed the performance program was changed to a subroutine of the main F-15 program and operated at a fixed rate of five samples per second. This was done to allow additional computer space for future usage.

Results of Modifications

The results of the modifications made to operate real-time are compared to the original post-flight program in Table 1 below. The most significant result was the calculation of thrust real-time with no loss in accuracy from the original post-flight program. This was a major improvement in flight test productivity and allows decisions concerning thrust output to be made in the control room.

TABLE 1: RESULTS OF MODIFICATIONS

ITEM	ORIGINAL	MODIFIED
Method of Data Reduction	Post-Flight	Real-Time
Time between test maneuver and data reduction	2-5 days	40 millisecs 1-2 hrs. hard copy
Program length	21 subroutines	12 subroutines
Accuracy (estimated)	2 to 5 percent	-- same --
Uncertainty calculation	Available	Not available
Output form	Lengthy hard copy with plotting available	Tabulated hard copy with plotting available, strip-charts

The delay in data reduction post flight was due to the time required to format the real-time flight data tape for use on the post flight Cyber computer. This delay varied with the work load and the availability of the real-time computer and had been longer than two weeks.

The improvement in flight-test productivity should help to relieve the work load on the engineer both during and after the flight since it provides a fast and accurate measure of engine performance for

immediate use. This should also reflect in a substantial financial savings by allowing important decisions concerning present and future flights to be made with no delay in obtaining performance data. Thus, problems in the past that would terminate or postpone flights can now be solved faster and sometimes immediately. This results in a savings of man hours, aircraft downtime and money.

Real-Time Data System

The actual F-15/DEEC real-time data system used to calculate thrust is shown in Figure 5. Data from the engine and airframe was captured at various rates and continuously telemetered to the ground station receiver. The raw data was recorded on a digital tape for future processing and supplied to the real-time computer for engineering units conversions and data reduction. The computer then supplied the output to the appropriate device.

Output was displayed real-time, every second on the CRT's and updated instantly on stripcharts in the control room. Hard copy was provided in table form shortly after any flight with plotting available directly after any maneuver.

In addition to this real-time thrust program a version of the original deck has been modified to run post-flight from the flight data base tape (FLIDAB). This program was used as a comparison and check to the real-time version and gave a detailed account of all thrust dependent parameters and uncertainties.

Implementation and Testing

Implementation of the real-time thrust calculation was accomplished during Phase 3 of the DEEC test program. Because this was a supplementary project, the initial data was used to verify the accuracy

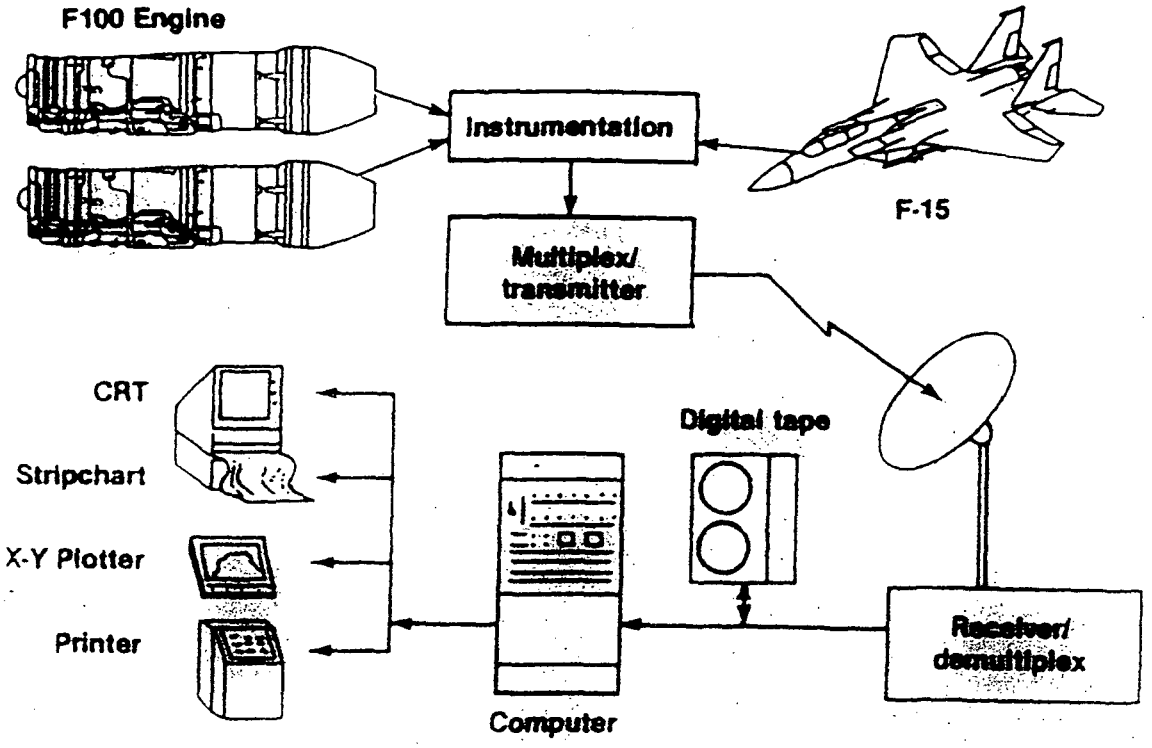

Figure 5. F-15 DEEC Real Time Data System

of the real-time program with the original post-flight version. This occurred with no disruption to the DEEC flight test program. Once verification was established, subsequent flights were made to take advantage of this new software.

Pertinent real-time thrust data was obtained from level flight acceleration runs at various altitudes and test day conditions. Power settings were military and maximum afterburning. Table 2 below summarizes these test runs.

TABLE 2: TEST RUN SUMMARY

FLIGHT	DATE	POWER SETTING	ALTITUDE	TERMINATING MACH NO.
412	1/10/83	MIL	5	.97
			10	.97
			20	.99
			30	.98
			40	.99
		MAX	10	1.24
			20	1.46
			30	1.94
			40	2.28

Because of the real-time program, thrust data was continually monitored on computer terminals and stripcharts in the control room. This allowed instant evaluation of steady-state thrust output as well as various unsteady conditions such as throttle transients, formation flight, and changes in attitude. In addition to gross and net thrust for both the TTW and PTA method, specific fuel consumption, total engine pressure ratio (PT7/P0) and ram drag were available for analysis.

RESULTS AND DISCUSSION

Samples of the results obtained from real-time data are shown graphically in Figures 6 through 9. These include steady and unsteady engine conditions and parameters of interest to the test and evaluation engineers. These plots were generated post-flight for illustrative purposes but represent actual real-time data.

Steady State Acceleration Runs

Two level acceleration runs at 30,000 feet were made during flight number 412 of the DEEC program. These two runs were made back-to-back and represent similar test day conditions. The first of these runs was a military power acceleration run. This was followed by a maximum power, full-after-burning acceleration run.

Figures 6 and 7 are plots of gross thrust versus Mach number for the two runs. Both plots illustrate the general tendency for the two gas generator methods to converge to the same thrust values as the run proceeds. This was probably due to the transition from unsteady to steady engine conditions during the initial part of each run since calibration of the two methods was made only at steady-state operating conditions.

Time histories of the gross thrust and the parameters fuel flow, ram drag and pressure ratios are shown in Figure 8 for the 30,000 feet, maximum power acceleration. At the start of this acceleration, the greatest disagreement between the two gas generator methods is noted.

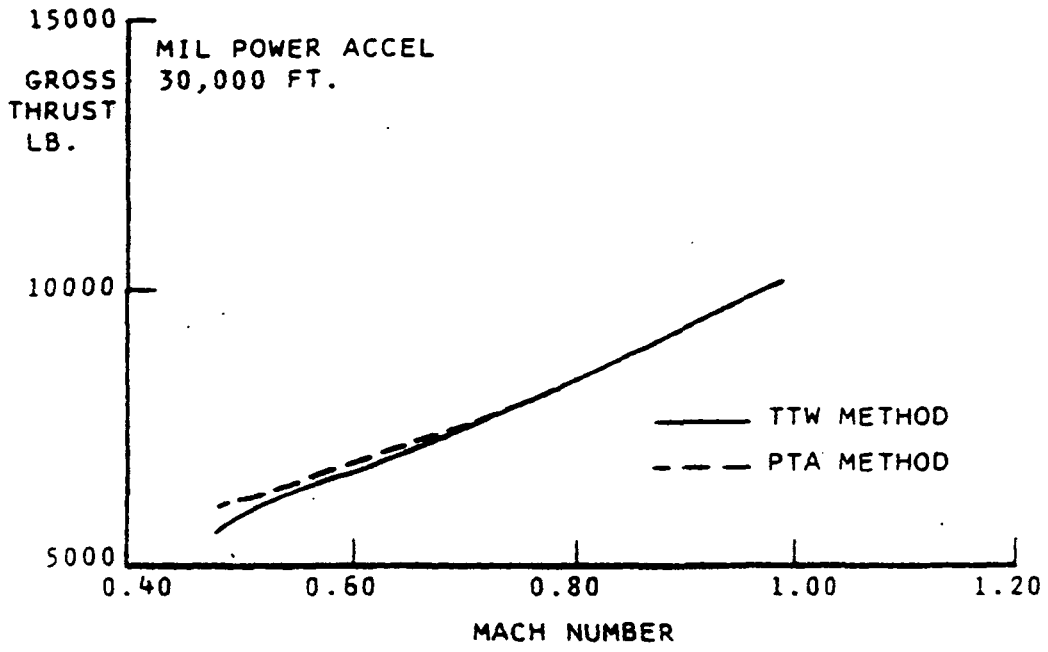

Figure 6. 30K MIL Power Acceleration (Thrust vs. Mach Number)

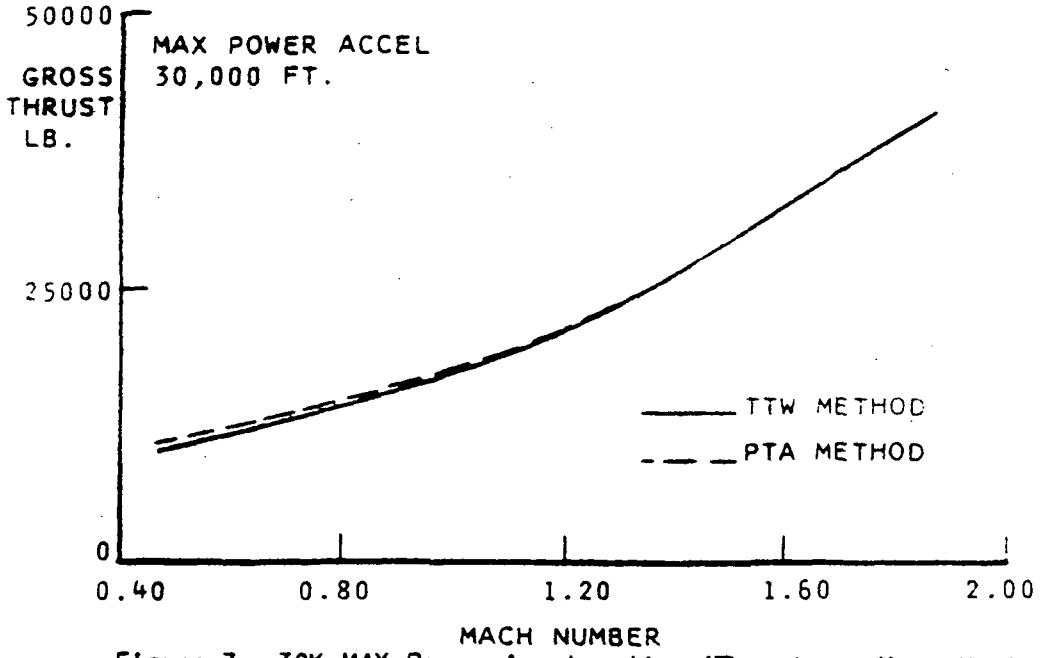

Figure 7. 30K MAX Power Acceleration (Thrust vs. Mach Number

This is the result of the engine operating at an unsteady state condition. The engine is reacting to the initial increase in power setting and its corresponding increase in airflow and fuel supply. As the run proceeds and the engine approaches a more stable operating condition the two methods converge toward the same thrust values.

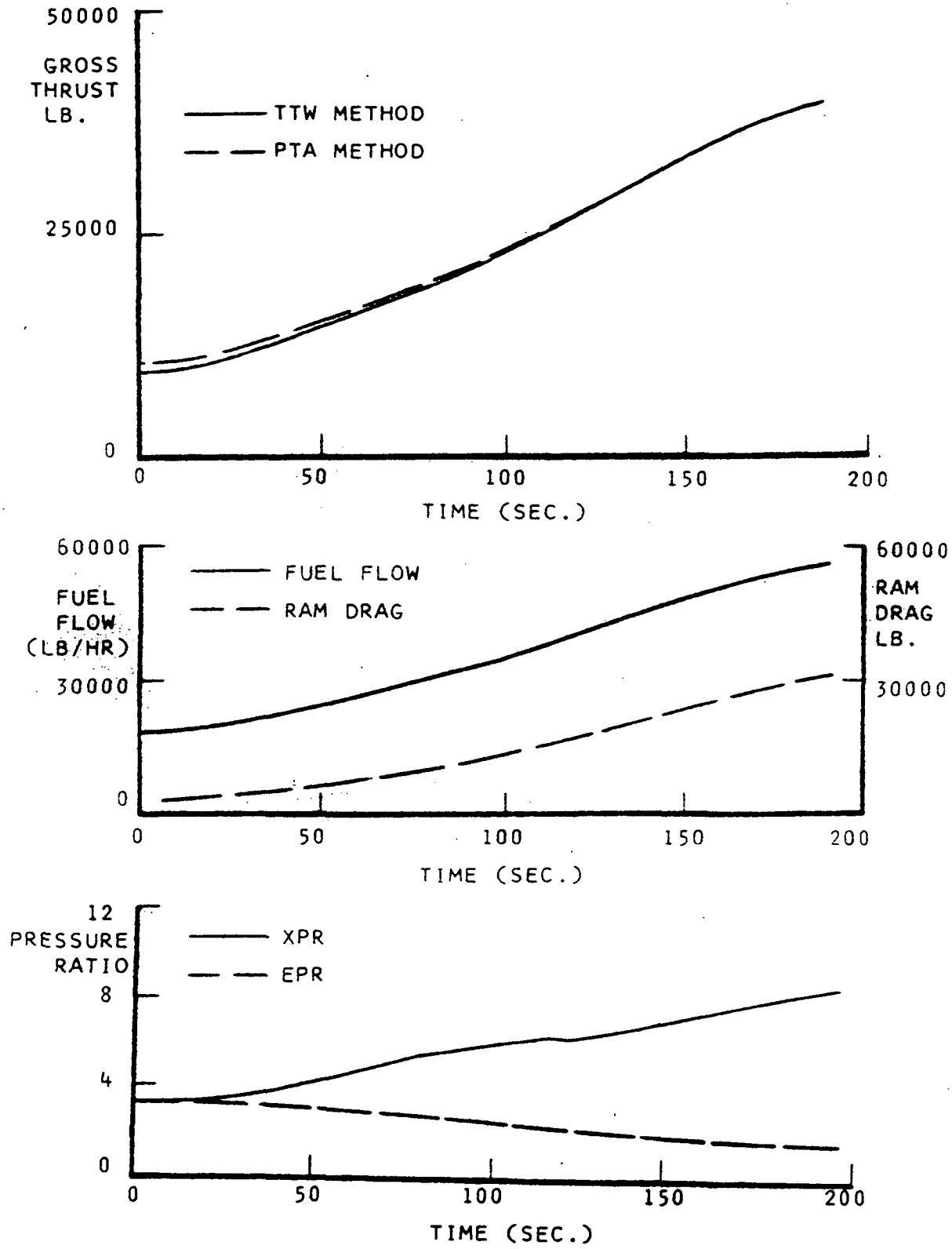

Figure 8. 30K MAX Power Acceleration (Time History)

The two pressure ratios shown in Figure 8 represent engine pressure ratio (EPR = PT6/PT2) and nozzle pressure ratio (XPR = PT7/PT0). Nozzle pressure ratio is an important parameter in both gas generator calculations and increases with thrust as expected. Engine pressure ratio decreases due to the relatively large increase in compressor inlet pressure (PT2).

All runs showed an increase in performance, particularly in maximum thrust, over standard F100 engines. This is also indicated by an increase in acceleration. Augmented net thrust was much greater than primary net thrust at all altitudes, ranging from 2 to 3.5 times these values. In general, net thrust increased with Mach and decreased with altitude. Fuel consumption showed similar tendencies with augmented fuel consumption ranging 5 to 6 times greater than maximum non-augmented fuel consumption. Engine fan rotor speed was relatively constant during the acceleration runs with very little differences between the corresponding values at military and maximum power. These results agree closely to the predicted performance values given in Reference 10 for standard day conditions.

Unsteady Throttle Settings

In addition to the acceleration runs, time history plots of a variety of transient throttle settings were made to evaluate the agreement between the two gas generator methods during unsteady engine operations. The results, shown in Figures 9, indicate good correlation for this case. The correlation was significant since the performance deck was intended for steady state engine operations and not calibrated in a dynamic environment. These plots also gave an important measure of the response time of the engine and indicate a slight time lag between

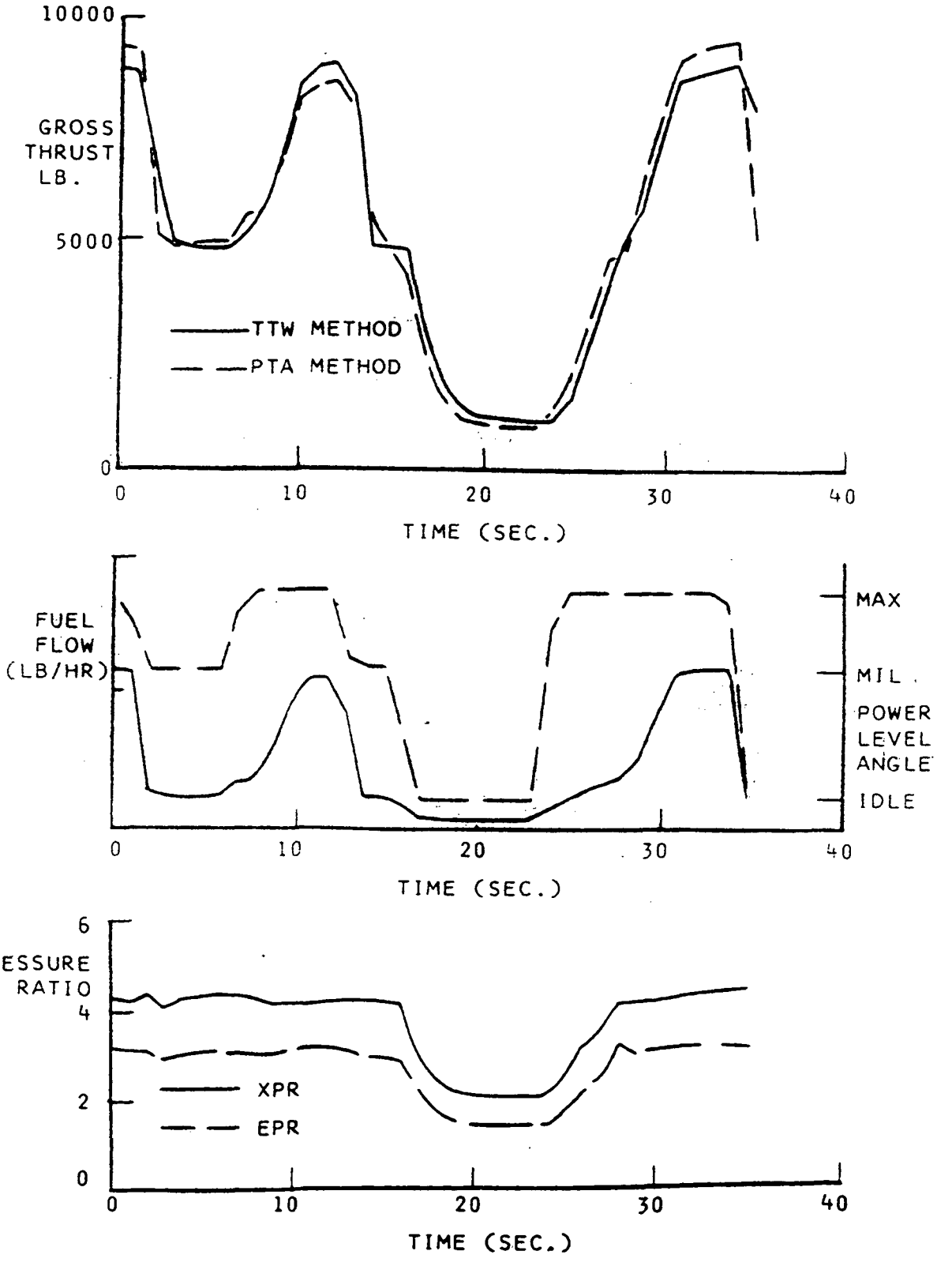

Figure 9: Unsteady State Throttle Transient (Time History)

throttle input and thrust output. This lag in response time could be very important to the safe operation of the aircraft, particularly when quick dynamic responses are required such as during formation flight.

Near Real-Time Thrust Plots

To aid in the performance analysis during a test flight, hard copy plots such as the one shown in Figure 10 were available shortly after any maneuver. This plot illustrates a 30,000 foot acceleration run at military power. The difference between the two methods at the beginning of the test run could be due to non-stable engine conditions. This represented a case in which real-time thrust computation data could be used by the test engineer to request a repeat of the acceleration run to obtain closer agreement between the two methods.

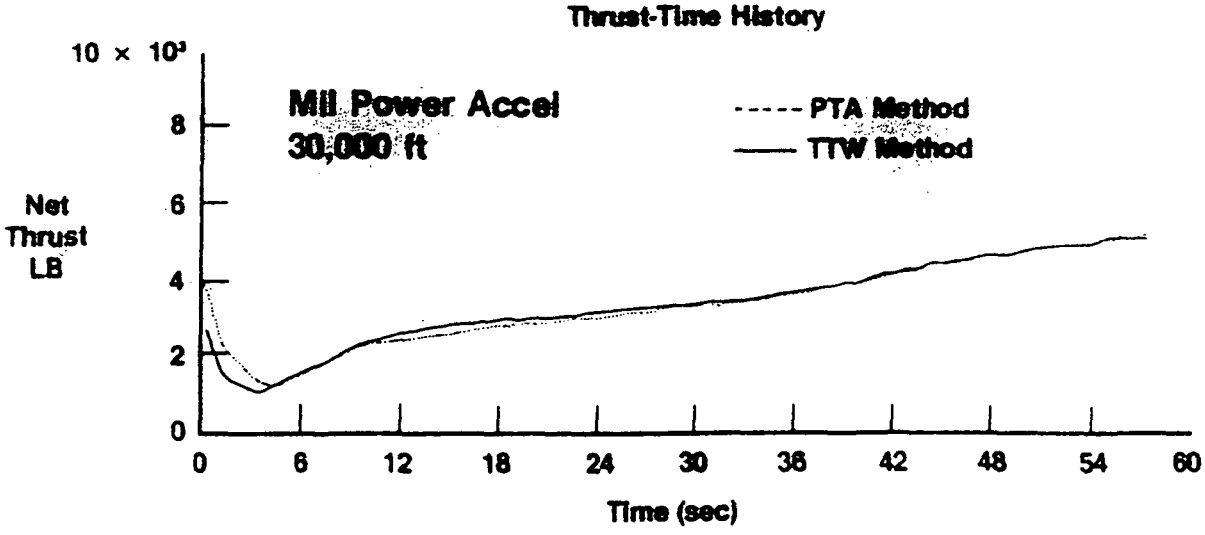

Figure 10. Near Real Time Thrust Time History

Accuracy and Uncertainty

The accuracy of the actual gross thrust calculation was primarily dependent on three factors: (1) the accuracy of the input data, (2) the

accuracy of the thrust model and (3) the accuracy of the calibration coefficients. Reference 7 found the model gross thrust uncertainty to be as high as 5.2 percent, but generally below 3.8 percent during altitude facility calibrations. The uncertainty dropped substantially with increasing thrust. The facility test also found the overall agreement between cell-measured thrust and calculated thrust for engine P680063 to be -1.5 percent for gross thrust (Reference 6). The results were less than $\pm$.8 percent for the maximum attainable power for each test condition again showing marked increase in accuracy with increasing thrust.

Because it was impossible to directly measure in-flight thrust, a comparison was made between the two calculated thrust methods and the predicted thrust from the engine manufacturer's simulation deck, Reference 11. The result is shown graphically in Figure 11 for a 40,000 foot, maximum power-acceleration run. Predicted thrust was calculated using a minimum of input such as test day altitude, Mach number, temperature and ram air recovery. With this limited input the simulation deck completely modeled all the major engine components including the fan, compressor, combuster, turbines, afterburner and nozzle. This accumulated data was used to calculate overall engine performance.

The agreement between the predicted and real-time calculated thrust was within two to five percent of each other. The predicted thrust was almost a constant 400 lbs. less than the real-time data except at the beginning of the run. This was because the empirical data tables within the simulation deck were obtained from a degraded F-100 engine and did not completely predict the full thrust output of a normal

engine. The overall results gave confidence to the accuracy of the real-time thrust calculation.

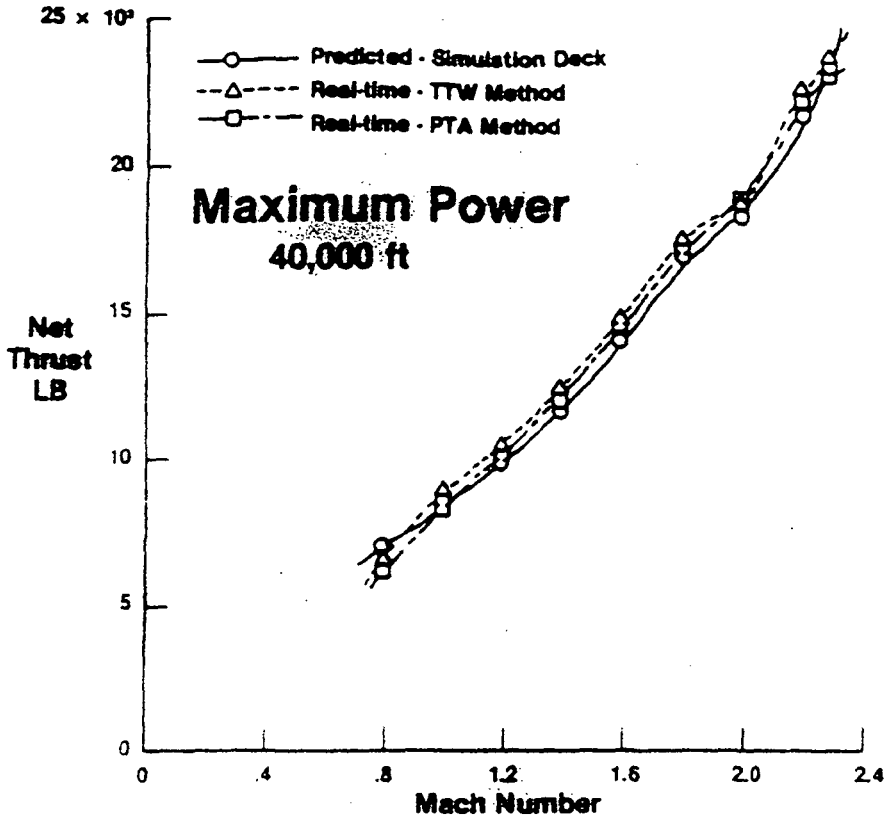

Figure 11. Predicted vs. Calculated Net Thrust

To further evaluate the accuracy of the data a comparison was also made between the predicted uncertainty of the manufacturer's original thrust deck (Reference 3) and the percent difference in thrust between the two methods. The results obtained for the 30,000 foot, maximum power acceleration run discussed previously are shown in Figure 12. The predicted uncertainties are based on a root mean square calculation of thrust uncertainty due to the uncertainty in input parameters:

$$U = \sqrt{[U(PTA)]^2 + [U(TTW)]^2}$$

$$U = \sqrt{\Sigma_i [U_i(PTA)]^2 + \Sigma_i [U_i(TTW)]^2}$$

where

$$U_i = (FG_i - FG)/FG * 100\%$$

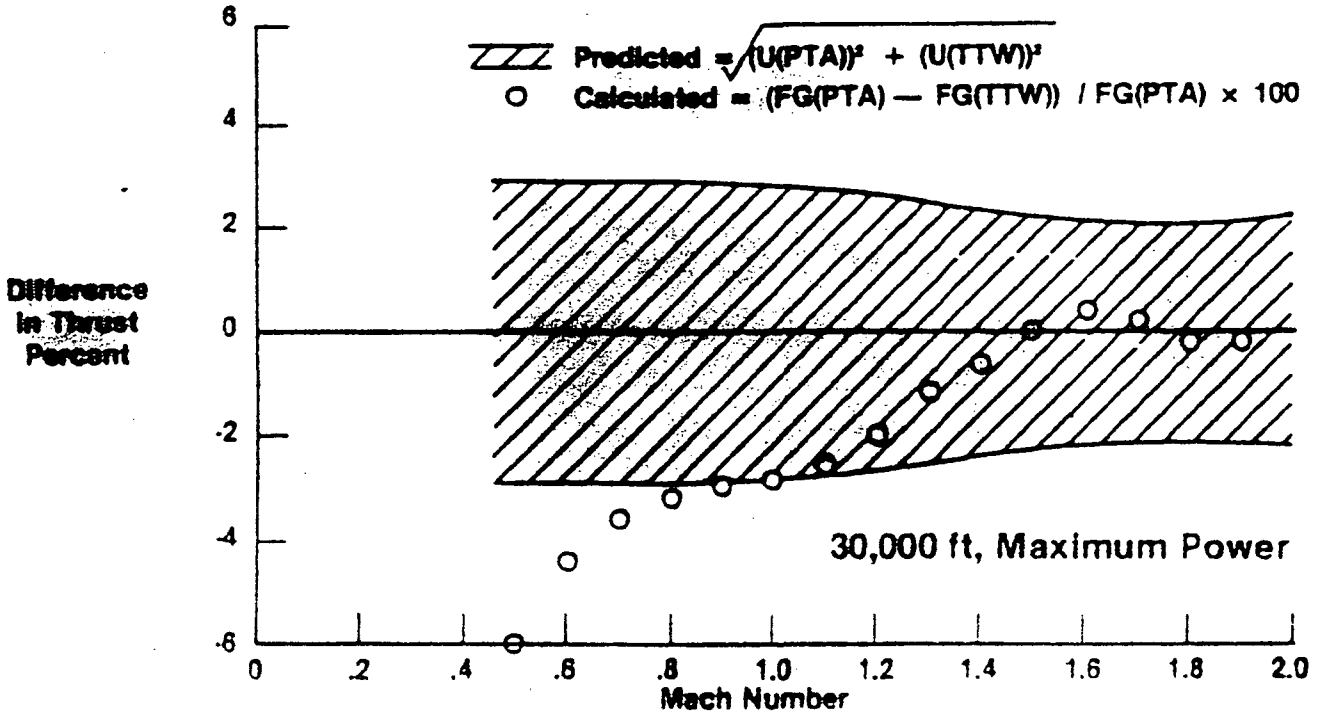

Figure 12. Difference Between PTA and TTW Calculated Thrust and Predicted Uncertainty

The uncertainty of each method, given by the root-sum-square combination of the independent thrust uncertainties. U_i is the percentage sum of the difference between the actual calculated thrust and the uncertainty thrust FG_i. The uncertainty thrust values were calculated by independently varying each input parameter by its uncertainty. The uncertainty of the independent variables is given in Table 3 along with the resulting calculated gross thrust uncertainty for a

TABLE 3

Parameter and Gross Thrust Uncertainty for the PTA and TTW Thrust Measurement Methods

Altitude (feet)	Power Setting	Mach Number	Parameter Uncertainty (%)						Gross Thrust Uncertainty (%)		
			PT7	PT0	AJ	T7	WG	WAT	U(PTA)	U(TTW)	U
10K	MIL	0.444	0.470	0.100	3.215	1.370	1.200	1.00	3.38	1.38	3.65
10K	MIL	0.977	0.372	0.100	3.082	1.384	1.200	1.00	3.32	1.34	3.58
10K	MAX	0.395	0.504	0.100	2.713	0.757	1.200	1.00	2.48	1.85	3.01
10K	MAX	1.256	0.354	0.100	1.864	0.651	1.200	1.00	1.75	1.50	2.30
30K	MIL	0.497	0.770	0.100	3.285	1.397	1.200	1.00	3.75	1.80	4.16
30K	MIL	0.992	0.558	0.100	3.231	1.368	1.200	1.00	3.62	1.50	3.92
30K	MAX	0.443	o.918	0.100	3.140	1.303	1.200	1.00	2.25	1.90	2.94
30K	MAX	1.892	0.388	0.100	1.836	0.643	1.200	1.00	1.63	1.41	2.15
40K	MIL	0.600	1.002	0.100	3.227	1.443	1.200	1.00	3.98	1.95	4.43
40K	MIL	0.802	0.923	0.100	3.237	1.433	1.200	1.00	3.78	1.73	4.16
40K	MAX	0.493	0.820	0.100	3.262	1.387	1.200	1.00	2.48	2.00	3.18
40K	MAX	0.825	0.922	0.100	2.519	0.666	1.200	1.00	2.30	1.86	2.96
40K	MAX	1.201	0.711	0.100	2.444	0.641	1.200	1.00	1.94	1.63	2.53
40K	MAX	1.801	0.549	0.100	1.853	0.647	1.200	1.00	1.75	1.50	2.30
40K	MAX	2,272	0.424	0.100	1.878	0.643	1.200	1.00	1.62	1.48	2.19

variety of operating conditions. In general the uncertainties tended to decrease with increasing mach number, altitude and power setting.

The large difference between the two methods in Figure 12 at the beginning of the run may be due to the transient time required for the engine to stabilize at a steady-state condition. This was also the area of lowest thrust that was found during altitude testing to have the highest model uncertainty and the greatest deviation from measured thrust. Above Mach one the results were within the predicted limits of ± 2.5 percent and showed excellent agreement near the maximum thrust output. This agreed with the results found during altitude-facility testing.

Airplane Performance Time Line

The potential of real-time computing is almost unlimited. It's time and cost saving advantages have led NASA to pursue more and more capacity. Figure 13 shows how the real-time engine performance will eventually evolve to the goal of real-time aircraft performance. Ultimately there is a need to accurately calculate lift and drag real-time and correlate them to standard day conditions for comparison to wind tunnel and theoretical values. This breakthrough should set a precedent for future real-time computer applications. Implementation of a real-time performance program is an important step in this direction.

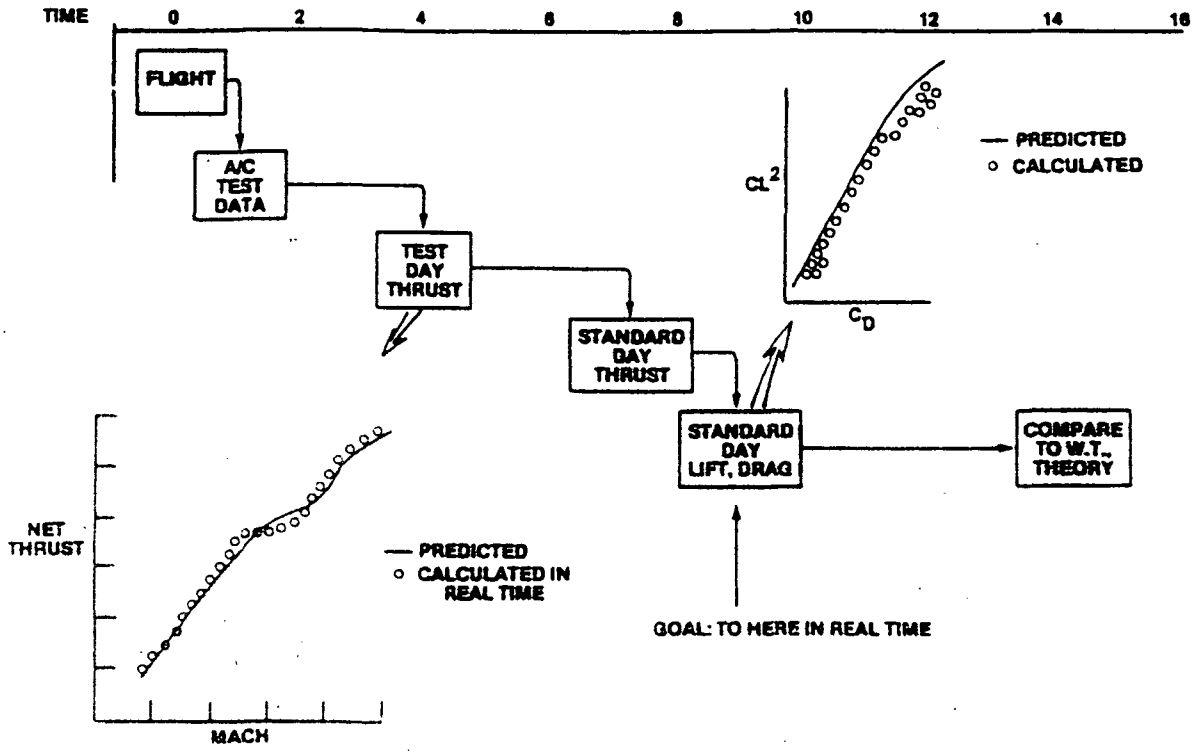

Figure 13. Airplane Performance Time Line

CONCLUSIONS

This thesis has verified the practicality and advantages of implementing a real-time inflight thrust calculation on the DEEC F100 Engine. The use of the DEEC computer greatly aided in the success of this project and allowed real-time thrust to be calculated with no loss in accuracy from previous post-flight methods. Results showed good agreement with previous predicted performance and uncertainty values and indicate an increase in accuracy with an increase in-flight mach number, altitude and power setting.

Real-time thrust was a major advancement in flight test productivity and efficiency by increasing aircraft diagnostics capabilities related to performance, resulting in decreased aircraft downtime and post-flight data reduction requirements. This should reflect a significant financial savings. The real-time thrust analysis has helped greatly in the performance analysis of the DEEC F100 engine and should eventually lead to more advanced aircraft performance programs setting a precedent for future test flight projects.

LIST OF REFERENCES

1. Arnaiz, Henry H.; and Schweikhard, William G.: Validation of the Gas Generator Method of Calculating Jet-Engine and Evaluation of XB-70-1 Airplane Engine Performance at Ground Static Conditions. NASA TN-D-7028, 1970.

2. Burcham, Frank W., Jr.: An Investigation of Two Variations of the Gas Generator Method to Calculate the Thrust of the Afterburning Turbofan Engines Installed in an F-111A Airplane. NASA TN-D-6297, 1971.

3. F100(3) In-Flight Thrust Calculation Deck, CCD 1088-3.0. Pratt and Whitney Aircraft, 1975.

4. Sams, H.: F-15 Propulsion System Design and Development. MCAIR Report 75-013, presented at the AIAA 7th Aircraft Systems and Technology Meeting at Los Angeles, California, 4-7 August, 1975.

5. Lancaster, Lanny T.G., and Eshbach, Russel E.: The F-100 Engine. SAE Technical Paper 801110, presented at the Aerospace Congress and Exposition, 13-16 October 1980.

6. Biesiadny, Thomas J.; Lee Douglas; and Rodriguez, Jose R.: Altitude Calibration of an F100, S/N P680063, Turbofan Engine. NASA TP-1228, 1978.

7. Kurtenbach, Frank J.: Comparison of Calculated and Altitude-Facility-Measured Thrust and Airflow of Two Prototype F100 Turbofan Engines. NASA TP-H-1015, 1978.

8. Myers, L.; Mackall, K.; and Burcham, F.W.: Flight Test Results of a Digital Electronic Engine Control System in an F-15 Airplane. AIAA-82-1080, presented at the AIAA/SAE/ASME 18th Joint Propulsion Conference, Cleveland, Ohio, 21-23 June, 1982.

9. Carpenter, T.W.; Levin, R.; and Ray, R.: Feasibility of Thrust Measurement During Flight of an Aircraft. California Polytechnic State University, San Luis Obispo, California, July 1981.

10. Horvat, Glen M.; and Myers, Lawrence: Predicted Performance of a Digital Electronic Engine Control System on an F100-PW-100 Engine in an F-15 Airplane. NASA NFRF Propulsion Brancgh Report 81-2, July, 1981.

11. F100 Model Derivative Program Users Manual for Deck CCD 1148-0.0. Pratt and Whitney Aircraft, 1980.